GNSS Shadow Matching: The Challenges Ahead

Paul D Groves, Lei Wang, Mounir Adjrad, Claire Ellul
University College London, United Kingdom

BIOGRAPHY

Dr Paul Groves is a Lecturer (academic faculty member) at University College London (UCL), where he leads a program of research into robust positioning and navigation within the Space Geodesy and Navigation Laboratory (SGNL). He joined in 2009, after 12 years of navigation systems research at DERA and QinetiQ. He is interested in all aspects of navigation and positioning, including improving GNSS performance under challenging reception conditions, advanced multisensor integrated navigation, and novel positioning techniques. He is an author of more than 70 technical publications, including the book *Principles of GNSS, Inertial and Multi-Sensor Integrated Navigation Systems*, now in its second edition. He is a Fellow of the Royal Institute of Navigation and holds a bachelor's degree and doctorate in physics from the University of Oxford. (p.groves@ucl.ac.uk)

Dr Lei Wang recently completed his PhD at UCL on GNSS shadow matching. He has won a number of awards for his research, including the Institute of Navigation's prestigious Parkinson Award for his PhD thesis in 2015. He received a Bachelor's degree in Geodesy and Geomatics from Wuhan University in 2010 and currently works for Microsoft.

Dr Mounir Adjrad is a Postdoctoral Research Associate at UCL. His current research interests are on Intelligent Urban Positioning (IUP) exploiting conventional GNSS technology augmented by urban environments 3D models. He has a multidisciplinary research experience in industry and academic institutions working on topics such as ultra-wideband technology, GNSS, satellite engineering, radar, biomedical engineering and transport engineering He holds a State Engineering degree in electronics, Magister in signal and communication, and State Doctorate in signal and systems from Ecole Nationale Polytechnique d'Alger, Algeria.

Dr Claire Ellul is a Lecturer at UCL, specializing in Three-Dimensional Geographical Information Science (3D GIS), with a particular interest in 3D usability – including rendering and analytical (topological) performance of large 3D city models on mobile devices and real-world applications of 3D GIS. Prior to becoming an academic, she spent 10 years as a GIS consultant and systems integration specialist.

ABSTRACT

GNSS shadow matching is a new technique that uses 3D mapping to improve positioning accuracy in dense urban areas from tens of meters to within five meters, potentially less. This paper presents the first comprehensive review of shadow matching's error sources and proposes a program of research and development to take the technology from proof of concept to a robust, reliable and accurate urban positioning product. A summary of the state of the art is also included.

Error sources in shadow matching may be divided into six categories: initialization, modelling, propagation, environmental complexity, observation, and algorithm approximations. Performance is also affected by the environmental geometry and it is sometimes necessary to handle solution ambiguity. For each error source, the cause and how it impacts the position solution is explained. Examples are presented, where available, and improvements to the shadow-matching algorithms to mitigate each error are proposed.

Methods of accommodating quality control within shadow matching are then proposed, including uncertainty determination, ambiguity detection, and outlier detection. This is followed by a discussion of how shadow matching could be integrated with conventional ranging-based GNSS and other navigation and positioning technologies. This includes a brief review of methods to enhance ranging-based GNSS using 3D mapping. Finally, the practical engineering challenges of shadow matching are assessed, including the system architecture, efficient GNSS signal prediction and the acquisition of 3D mapping data.

1. INTRODUCTION

The performance of global navigation satellite systems (GNSS) positioning in dense urban areas is poor because buildings block, reflect and diffract the signals. Those signals with lines of sight perpendicular to the street direction are more likely to be blocked or reflected by buildings than signals travelling along the street. Thus, the signal geometry, and hence the positioning accuracy, is much better along the direction of the street than across the street [1][2].

Positioning accuracy in the cross-street direction is of great importance to many applications. Examples include vehicle lane detection for intelligent transportation systems (ITS), location-based advertising, augmented-reality, and step-by-step guidance for the visually impaired and for tourists. Augmenting GNSS with other sensors can improve the position solution availability and robustness, but does not particularly improve the cross-street accuracy. A possible solution arises from the increasing availability of 3D city models, which enable the effects of the buildings on GNSS signal propagation to be predicted [3][4].

GNSS shadow matching is a new technique that determines position by comparing the measured signal availability and strength with predictions made using a 3D city model [1]. It is designed to be used alongside conventional ranging-based GNSS positioning in dense urban areas to improve the cross-street accuracy. The basic principles are described in Section 2. Since 2011, several research groups have demonstrated shadow matching experimentally, using both single and multiple epochs of GNSS data. Cross-street positions within a few meters have been achieved in environments where the error in the conventional GNSS position solution is tens of meters, enabling users to determine which side of the street they're on. Shadow matching has also been demonstrated in real time on an Android smartphone. This work is reviewed in Section 3.

The potential of shadow matching to provide accurate positioning in dense urban areas has been proven. The challenge now is to make it sufficiently reliable and efficient for deployment in professional and consumer products. Thus, shadow matching must:

- Work across a wide range of different environments, not just a few carefully selected test areas;
- Provide reliable quality metrics to enable it to be appropriately weighted within an integrated navigation system;
- Be easily adapted to work across different designs of user equipment;
- Be efficient in its use of processing, data storage, and communications capacity;
- Have access to suitable 3D mapping at a viable price.

This paper therefore sets out the technical research and development challenges that must be met to take shadow matching from proof of concept towards a commercial product.

Section 4 presents the first comprehensive review of the sources of error in shadow matching, explaining each error and discussing how it might be mitigated through improvements to the shadow matching algorithms. Section 5 proposes approaches to quality control, comprising uncertainty determination and outlier detection, both of which are required for a robust positioning system. Section 6 discusses the integration of shadow matching with conventional ranging-based GNSS positioning and other sensors. Then, Section 7 discusses the practical engineering of shadow matching, including sourcing and dissemination of 3D building data, system architectures and efficient GNSS signal prediction. Finally, Section 8 presents a summary of the research and development tasks that are required to take shadow matching to maturity.

2. THE BASIC CONCEPT

Shadow matching uses a 3D city model to predict where within a street signals from each satellite can be directly received. Consequently, by determining whether a direct signal is being received from a given satellite, users can localize their position to within one of two areas of the street. By repeating this process for several different satellites, a position solution can be determined. Figure 1 illustrates this.

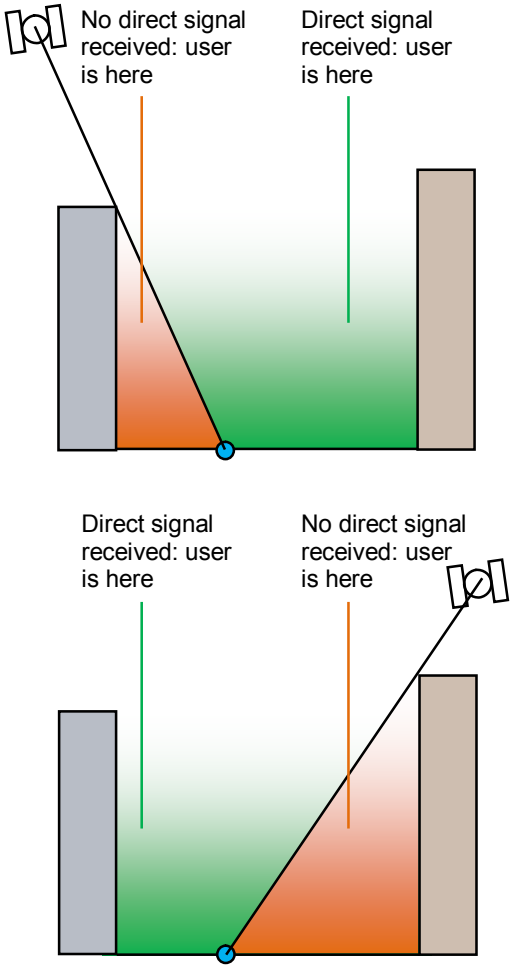

Figure 1: Principle of Shadow Matching.

In practice, a hypothesis testing approach is adopted, whereby an array of candidate positions are scored according to how well the predicted and measured satellite visibilities match. This enables errors in the matching process (see Section 4) to be treated as noise. Shadow matching uses a fundamentally different positioning method from conventional GNSS. Whereas conventional GNSS uses the ranging method, shadow matching uses pattern matching, also used in Wi-Fi received signal

strength (RSS) fingerprinting and terrain referenced navigation (TRN) [5].

Figure 2 shows a typical shadow matching algorithm, comprising five steps:

1) Firstly, a search area is determined using, for example, the conventional GNSS position solution and an appropriate confidence interval. Within this search area, a grid of candidate positions is set up.
2) For each candidate position, the satellite visibility is predicted either using the 3D city model directly or from pre-computed building boundaries (the minimum elevation above which satellite signals can be received at a series of azimuths) at each position. Satellite azimuths and elevation angles are obtained from the navigation data as for conventional GNSS positioning.
3) The observed satellite visibility is determined from the GNSS receiver's carrier-power-to-noise-density ratio, C/N_0, measurements. In a basic shadow matching implementation, a signal is assumed to be directly received if the signal is tracked and the C/N_0 measurement exceeds a certain threshold. Signals tracked with a lower C/N_0 are assumed to be reflected or diffracted, i.e. the direct path to the satellite is assumed to be blocked.
4) The next step is to score each candidate position according to the match between the predicted and measured satellite visibility. The simplest approach is to score one point for each matching satellite and zero for those satellites that do not match. These scores may be depicted as a map, as shown later in the paper.
5) Finally, a position solution is derived from the matching scores of all of the candidate positions. A simple approach is to average the positions of the highest scoring candidates.

To get the best performance out of the shadow-matching technique, each of these five steps must be optimized.

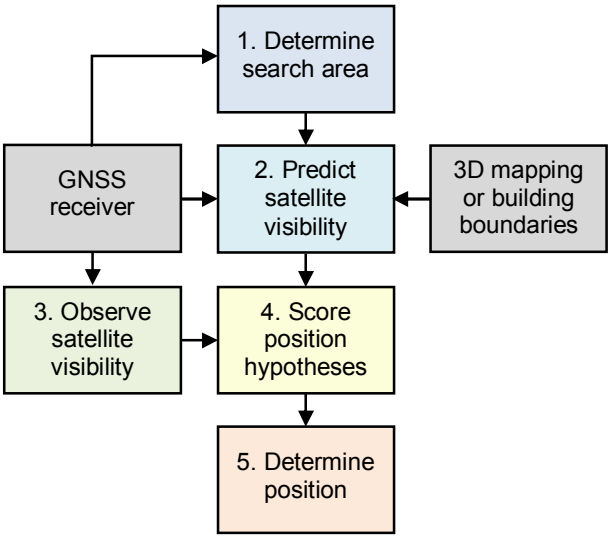

Figure 2: A Typical Shadow Matching Algorithm

3. A BRIEF HISTORY OF SHADOW MATCHING

The shadow matching concept was independently conceived by four different research groups [6][7][1][8], each publishing before becoming aware of the work of the others. In [7], the concept is extended to matching the predicted and measured C/N_0. The term 'shadow matching' was first introduced in 2011 [1], with the first experimental results quickly following. Tests of a full shadow matching algorithm are briefly summarized in [8], with an average error of 4m reported for a single-epoch implementation and an accuracy within 1m achieved for observations over several hours. A simpler shadow matching experiment using a geodetic multi-constellation GNSS receiver is described in detail in [9]. In these tests, shadow matching identified the user to be on the correct side of the street more than 97% of the time and distinguished the footpath from a vehicle lane 90% of the time. A *GPS World* publication at the beginning of 2012 then brought shadow matching to a wider audience [10].

Following the initial proof of concept, a wide range of tests have been published with different shadow-matching algorithm designs spanning static, pedestrian and vehicle; single and multiple epochs; and with different classes of GNSS receiver. Static testing of a full single-epoch shadow-matching algorithm at multiple sites using a geodetic GNSS receiver is described in [11]. In these tests, the cross-street positioning error was within 5m for 89% of the time and within 2m for 64% of the time. The utility of predicting diffracted signals was also investigated. In [12], it was shown that a consumer-grade GPS chip with a geodetic-grade antenna can achieve an RMS error of 4m at a site where the building geometry allows shadow matching to work in two dimensions.

Multi-epoch static positioning using a particle filter was demonstrated in [13]. Here, reflection and diffraction of the GNSS signals was also modelled and convergence of the position solution to within 2m was achieved after 32s of data.

The first smartphone shadow matching results were presented in [14], closely followed by a real-time demonstration [15]. A direct comparison of smartphone and geodetic receiver shadow matching across 20 sites using the same algorithm showed that the geodetic receiver is almost twice as accurate as the smartphone in the cross-street direction [16]. This is primarily due to the antenna characteristics, as discussed in Section 4.7. To mitigate this, the shadow matching algorithm was adapted to treat the measured satellite visibility as fuzzy, with the probability of the received signal being direct modelled as a function of the C/N_0 measurement [16][17].

In [18], it was shown that shadow matching can be used for road lane identification in relatively open areas by making use of the shadows cast by mobile phone masts. However, receiver firmware modifications are needed to

detect these at speed because C/N_0 measurement with a high spatial resolution are needed.

Recently, several research groups have demonstrated multi-epoch shadow matching for a moving pedestrian using a particle filter [19][20][21][16][22]. In tests with smartphone data, the cross-street accuracy was 12.8m using conventional GNSS, 4.6m using single-epoch shadow matching and 2.2m using the particle filter [16]. Meanwhile, the first three dimensional shadow matching algorithm was demonstrated by simulation in [22].

Finally, a number of researchers have demonstrated the reverse process of building a 3D city model using GNSS measurements [23][24][25][26]. In [19][20], shadow matching and map building were combined into a simultaneous localization and mapping (SLAM) process.

4. ERROR SOURCES AND THEIR MITIGATION

GNSS shadow matching and conventional GNSS positioning operate on different physical principles. Shadow matching applies the pattern matching positioning method to C/N_0 (or signal-to-noise) measurements, whereas conventional GNSS positioning applies the ranging method to pseudo-range measurements [5]. Consequently, their error sources are very different. The satellite clock, ephemeris, ionosphere and troposphere propagation errors that impact conventional GNSS positioning have very little impact on C/N_0 measurements (apart from ionospheric scintillation), so do not affect shadow matching. Shadow matching is affected by multipath, non-line-of-sight reception, radio frequency interference and signal attenuation. However, these affect C/N_0 and ranging measurements differently. Finally, there are many error sources which impact shadow matching, but not conventional GNSS positioning.

Shadow matching step	Initialisation	Modelling	Propagation	Environmental complexity	Observation	Algorithm approximations
1. Determine search area	✓					
2. Predict sat. visibility		✓	✓	✓		
3. Measure sat. visibility					✓	
4. Score pos. hypotheses						✓
5. Determine position						✓

Table 1: Mapping of error sources to shadow matching algorithm steps

This section reviews all of the (known) sources of error in shadow matching. It discusses their causes, describes how they impact the position solution and presents examples, where available. Improvements to the shadow-matching algorithms to mitigate these errors are also proposed. Error sources may be divided into six categories: initialization, modelling, propagation, environmental complexity, observation, and algorithm approximations. Table 1 shows which error sources affect each stage of the shadow matching process (Figure 2).

The section begins with a discussion of environmental geometry, loosely equivalent to solution geometry and dilution of precision in ranging. This is followed by an introduction to ambiguity. Each error source is then discussed in turn. A review of position determination methods is included within Section 4.8.

4.1 Effect of Environmental Geometry

The accuracy of a shadow-matching position solution is affected by the environmental geometry in three ways: building distribution, building height to street width ratio, and scale. Street direction also has an effect because of the orbital distribution of the GNSS satellites. Figure 3 shows two different ways in which buildings may be distributed in dense urban areas. Where there are high-rise towers with large gaps between the individual towers, the GNSS signal shadowing will vary in both the along-street and cross-street directions, enabling a two dimensional position solution to be obtained from shadow matching [8][13].

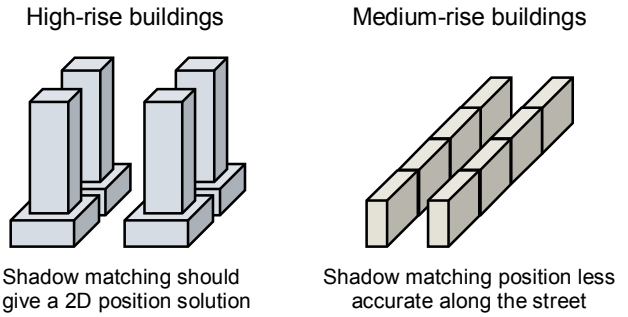

Figure 3: Building distributions in urban areas

In older urban areas comprising medium-rise buildings (and often narrower streets), the gaps between adjacent buildings are too narrow to allow GNSS signals through, resulting in little variation in signal shadowing along the street. In these areas, accurate shadow matching is generally limited to the cross-street direction, along which conventional GNSS is less accurate [2]. Figure 4 illustrates this with a shadow-matching scoring map based on smartphone measurements. The algorithm configuration is described in [17] and the scores are normalized to a scale of 0 to 1. The highest-scoring area (shown in dark red) is on the correct side of the street, but extends for a long distance along the street, so there is a large position uncertainty in the along street direction. Figure 5 shows a similar scoring map for a user located near a junction. Here, the highest-scoring area is much smaller.

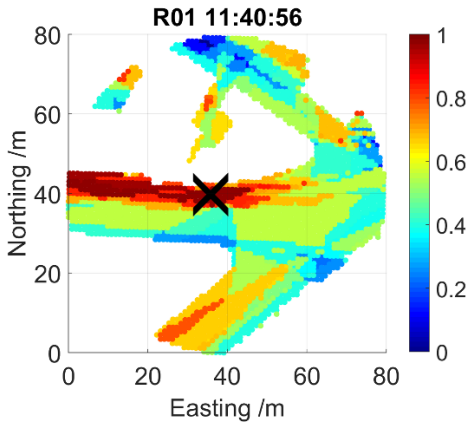

Figure 4: GNSS shadow-matching scoring map for a mid-street location with no large gaps between buildings (the cross shows the true position and white areas are indoor locations)

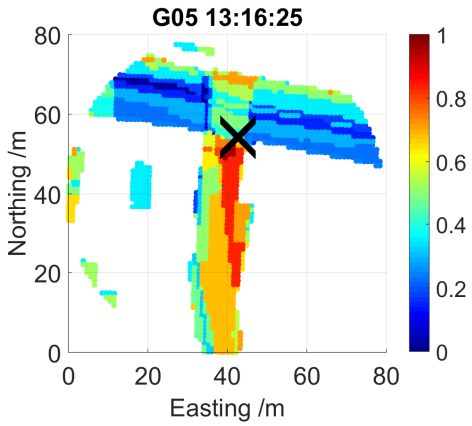

Figure 5: GNSS shadow-matching scoring map for a location near a road junction (the cross shows the true position and white areas are indoor locations)

The next environmental geometry factor that affects shadow-matching performance is the building height to street width ratio. Shadow matching relies on there being satellites that are directly visible in some parts of the street and blocked by buildings in others. The more of these partially visible satellites there are, the more accurate and reliable shadow matching should be. If the building height to street width ratio is low, the environment will be open and most satellites will be directly visible except very close to buildings. Shadow matching will not work well under these conditions; it will only be able to determine when the user equipment is close to a building. However, as conventional GNSS positioning works well in open environments, this is not a problem. Conversely, if the building height to street width ratio is high, most satellites will be blocked at all candidate positions, leaving only a few available for shadow matching. Adding reflected signal prediction (see Section 4.5) to the shadow-matching concept should improve performance under these conditions, as should the increase in the number of GNSS satellites as Galileo and Beidou development continues.

Simulations have been conducted to quantify the impact of building height to street width on shadow-matching performance [1]. These also highlighted a dependency on street direction, with fewer satellites directly visible in north-south streets than east-west streets (assuming a 45° latitude). Consequently, both conventional GNSS and shadow matching were predicted to work better in east-west aligned streets. The minimum building height to street width ratio tested was 0.5 as, below this, conventional GNSS was predicted to work well (assuming two constellations). As the building height to street width ratio increases above 0.5, shadow-matching performance was predicted to degrade with position errors roughly doubling at a height to width ratio of 1.5 for north-south streets and 3 for east-west streets. Experimental work is needed to verify these results.

The final environmental factor to consider is scale. For each partially visible satellite, the buildings divide the environment into regions where the signal can be directly received and regions where it cannot. The bigger the buildings and spaces between them, the larger these regions will be and the coarser shadow matching will become. The accuracy of an 'ideal' shadow matching system, ignoring modelling errors (Section 4.4) and signal propagation effects (Section 4.5) is thus directly proportional to the scale of the environment. The practical accuracy of shadow matching depends on many other factors, some of which vary with the scale of the environment and some of which do not. For example, the area over which a signal is affected by diffraction, blurring the boundary between shadowed and unshadowed areas, is proportional to the distance of the structure causing that diffraction. Similarly, if the 3D city model is represented as a set of building boundaries [2], the impact on positioning resolution of the boundary resolution depends on how far away the buildings are. Thus, a 1° azimuth resolution corresponds to a 0.35m positioning resolution for a building 20m away and a 1.75m positioning resolution for a building 100m away. Again, experimental work is needed to assess the practical impact of scale on shadow-matching performance.

4.2 Ambiguity in Shadow Matching

An inherent characteristic of all pattern-matching positioning techniques is that there is sometimes a good match between measurements and predictions at more than one candidate position. In GNSS shadow matching, ambiguity can occur when the building geometry is repeated at different locations within the search area such that the same combination of satellites is predicted to be visible at multiple non-contiguous locations. However, ambiguity can arise as a consequence of errors in the shadow-matching process. Thus, the score at the true position may be reduced, while the scores at some of the incorrect positions may be inflated. Figure 6 shows an example of an ambiguous shadow-matching scoring map based on smartphone measurements. The algorithm configuration is described in [17] and the scores are

normalized to a scale of 0 to 1. Maximum scores (shown in dark red) are obtained at several different locations within the search area, giving several possible position solutions.

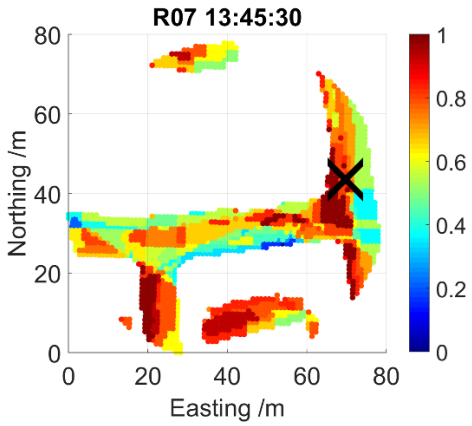

Figure 6: GNSS shadow-matching scoring map showing an ambiguous position solution (the cross shows the true position and white areas are indoor locations)

There are a number of ways of mitigating the ambiguity problem. These are not mutually exclusive, so can be deployed in combination. The possibilities are as follows:

1) Using positioning algorithms that are designed to handle ambiguity as discussed generically in [27] and for shadow matching in Section 4.8
2) Minimizing the search area; the fewer candidate positions under consideration, the less likely an ambiguous match will occur. However, this can also result in a wrong position, as discussed in Section 4.3.
3) Improving the accuracy of the scoring map through improvements to the whole shadow matching process, which is the focus of much of this paper. With fewer errors propagating through, the true position is more likely to score significantly higher than the other candidates.
4) Using more measurements, combining information from successive epochs and/or using additional GNSS constellations (when available). However, this only works where the errors in the position hypothesis scores are random, not when they are systematic. Experiments with four-constellation shadow matching (achieved by combining two separate datasets) showed no significant improvement over two-constellation results [17]. From this, it can be concluded that there are significant systematic errors that must be addressed.

4.3 Initialization Errors

The initialization phase of shadow matching uses external information, such as the conventional GNSS position solution, to determine the search area for the satellite visibility prediction and position hypothesis scoring phases. In experiments published to date (see Section 3), the search area has been defined as a fixed-radius circle or fixed-side square centered about the initialization position or the true position (which is not available in a practical system). This does not account for variation in the quality of the initialization information supplied to the shadow-matching algorithm.

If the search area is too big, the computational load will be larger than necessary and an ambiguous scoring map is more likely. Conversely, if the search area is too small, it will often exclude the true position, making a correct shadow matching solution impossible. Figure 7 illustrates this. Problems can also occur when the true position is right at the edge of the search area as it may be inadequately weighted within the position solution when there is ambiguity in the matching process.

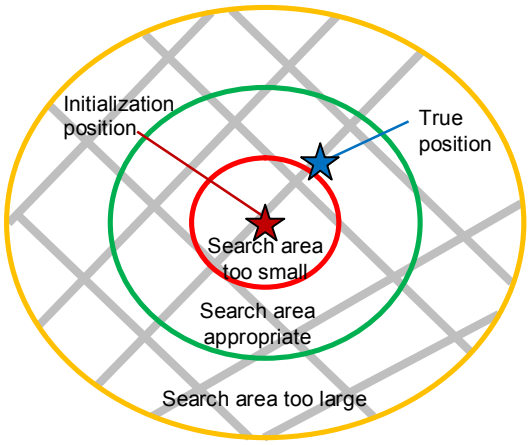

Figure 7: Shadow Matching Search Area Determination

Effective initialization of shadow matching therefore requires:

- Reliable position information from other positioning systems, i.e. no large outliers;
- Reliable information on the uncertainty of the positioning information;
- An algorithm that determines the optimum search area from the above information (and the mapping data).

If the size of the search area is scaled with the uncertainty of the initialization position, a fixed probability of the position being within the search area is maintained, so ambiguity is not introduced unnecessarily. For ranging-based positioning, such as conventional GNSS, the probability distribution of the initialization position depends on the signal geometry, so the position is more accurate in some directions than others [5]. Therefore, if the search area is approximated to a circle (or square), there will be both an increase in ambiguity and an increased chance of the true position lying outside the search area as shown in Figure 8. Therefore, it is important that the initialization position uncertainty is considered in two dimensions. This requires three parameters: either the semi-major axis size, semi-minor axis size and axis direction of the error ellipse, or the north position error variance, east position error variance, and north-east position error covariance.

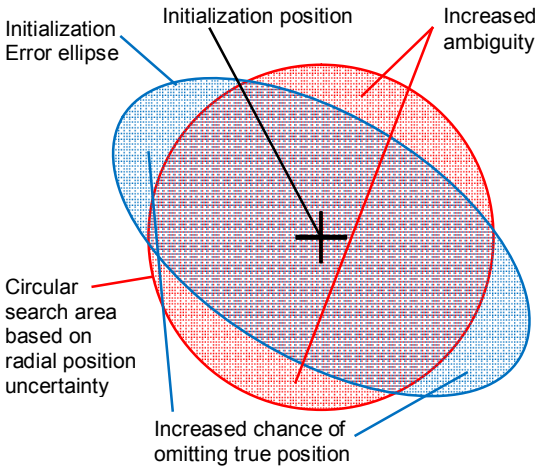

Figure 8: Effect of approximating the search area to a circle

A key problem with using conventional ranging-based GNSS for initialization is that the accuracy varies. In open areas, the horizontal position error is usually within 10m. In dense urban areas, position errors of a few tens of meters are typical, but much larger errors can occur when there is NLOS reception via a distant reflector. Commercial position solutions do not typically come with much quality information. Dilution of precision (DOP) values provide information on the solution geometry, but not the degree of multipath and NLOS contamination. Furthermore, it is not possible to know how the positioning algorithm deals with outliers.

The best way of minimizing these problems is for the shadow matching system to generate its own ranging-based GNSS solution so that the quality and uncertainty of that solution is well known. By using a 3D city model, it should also be possible to compute more realistic error bounds for that solution, though this requires further research. This is part of the intelligent urban positioning (IUP) concept [28], discussed in Section 6.1, in which the 3D city model can also be used to improve the accuracy of the ranging-based position solution. However, this all relies on the availability of GNSS user equipment that outputs pseudo-ranges (see Section 7.1).

Wi-Fi positioning is another possible source of initialization. Because buildings also block Wi-Fi signals, it should be better than GNSS at distinguishing between parallel streets. However, it is difficult to determine the quality and accuracy bounds of the solution as commercial Wi-Fi positioning software does not provide this information. Reliability also depends on how the Wi-Fi positioning algorithms work, how many access points are used, and how the database is created, all of which are kept confidential by the supplier. Empirically determining suitable uncertainty bounds for Wi-Fi position measurements as a function of the building geometry would require a large amount of experimental data.

For multi-epoch shadow matching, whether stand-alone, part of an IUP system, or part of a multisensor navigation system, the previous epoch's position solution is available for determining the search area for the current epoch. This is potentially the most reliable approach as it uses the most information, provided the algorithms correctly account for the solution ambiguity and motion between epochs. However, multi-epoch position is not suited to all applications of shadow matching.

4.4 Modelling Errors

The prediction phase of shadow matching uses a 3D city model to predict which GNSS signals are directly receivable at each candidate position within the search area. This requires an accurate city model, but it also requires an effective method for determining which buildings affect signal reception. The area containing these buildings is sometimes called the region of interest (ROI) [8]. If an ROI larger than necessary is used, the processing load will be increased. However, if the ROI is too small, important buildings will be omitted, resulting in blocked signals being predicted as direct line-of-sight (LOS), causing position errors. Errors due to "missing" buildings can potentially be compensated using outlier detection (Section 5.3). However, the number of outliers (from all causes) must be minimized as outlier detection does not work when there are too many errors.

Within the shadow-matching literature, there is currently no consensus on ROI size and shape. In [2][11][16][17], buildings within a 300m radius of each candidate position are considered, while the overall ROI is limited to 200×200m in [8] and 100×100m in [18]. In [13], buildings within 100m of each candidate are considered. These differences may reflect the characteristics of each research group's test site. Where all buildings are of a similar height, a relatively small ROI should suffice. However, buildings that are much taller than their neighbors will affect GNSS signal reception over a much wider area. A possible solution to this problem is to add ROI guidance to the city model. For example, each 10×10m tile could be accompanied by a set of coordinates defining the perimeter of the area containing those buildings which impact GNSS reception within that tile. Alternatively, the height of the tallest in each 50×50m tile could be used to determine whether to include that tile in the ROI.

CityGML (the Open Geospatial Consortium's approved standard for storage and exchange of virtual 3D city models, [29]) defines 3D city models as having varying levels of detail (LOD) [30]. LOD 0 is a digital terrain model, sometimes called a 2.5D model. LOD1 is a block model without any roof structures, i.e. all the buildings have flat roofs. Finally, LOD 2 is a full 3D city model having explicit roof structures and potentially associated texture.

City models are commonly stored using a boundary-representation approach, where each face (wall, floor,

roof) of a building is described separately and a collection of faces grouped to represent the building. To minimize storage, these can be represented as polygons, described by the coordinates of each node (corner point). However, due to rounding errors this may not result in planar faces, which can cause problems for some of the techniques used to predict GNSS signal propagation, such as ray tracing. Thus, polygons are frequently triangulated, either on the fly or as a pre-processing stage, and a triangular mesh created prior to visualization or further processing. The greater the level of detail, the greater the number of triangles and hence the greater the time required for triangulation and the computational complexity of subsequent steps. Figures 9 and 10 show two 3D models of the same area of London, with Figure 9 derived from LOD 1 data and Figure 10 derived from LOD 2 data.

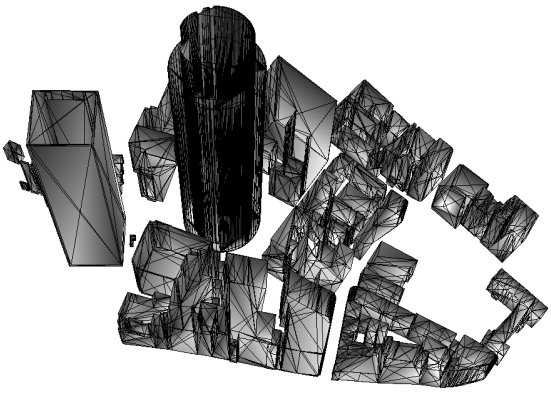

Figure 9: LOD 1 3D model of Central London near Fenchurch Street (data from Ordnance Survey)

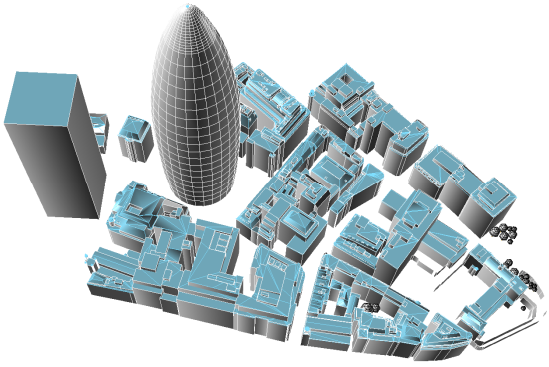

Figure 10: LOD 2 3D model of Central London near Fenchurch Street (data from Z Mapping)

Errors due to approximations in the city model directly lead to errors in the shadow matching solution. If a modelled building is displaced horizontally by 1m from its true position, the shadows it casts will also be displaced by 1m, so a shadow-matching position derived only from that building would be in error by 1m. In practice, multiple buildings are used, so the contribution to the shadow-matching position error will be a weighted average of the individual building displacements. Environmental geometry (Section 4.1) limits shadow matching precision to about 0.5m [1], while the physics of signal propagation at GNSS wavelengths may limit precision to 1–2m, as discussed in Section 4.5. Thus, a horizontal accuracy and resolution of 0.5m is a reasonable requirement to set for the city model.

LOD 1 city models represent roofs as flat, and are created by a process of 'extrusion' which builds these models by taking 2D buildings to a given height. The provided height may vary depending on the data source, and could be an average height for the rood, an eaves height or a ridge height. Furthermore, real roofs may be pitched, while flat roofs may include perimeter walls, lift shaft and stairwell heads and other furniture, such as fans and satellite dishes. Even many LOD 2 models may omit these features. In practice, any roof feature that is visible from the ground can impact (ground-level) shadow matching. Figure 11 shows some rooflines around London as viewed from street level, where a GNSS antenna would typically be. The visibility of roof details varies. The effect of roofline modelling on shadow matching is thus a subject for further study.

Figure 11: London rooflines viewed from the street below

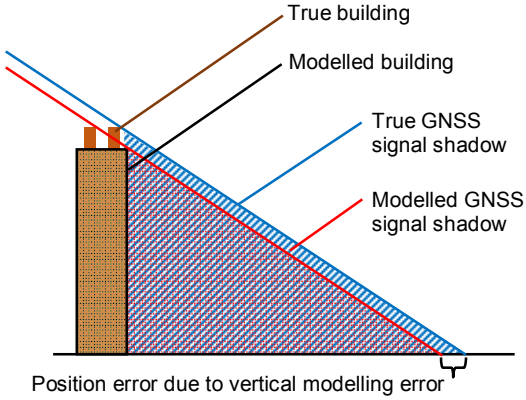

Figure 12: Impact of vertical model error on shadow position

The error in the shadow position due to a vertical error, δh, in the city model is $\delta h / \tan\theta$, where θ is the satellite elevation angle, as shown in Figure 12. Thus, shadow matching using low-elevation satellites is more

susceptible to roof modelling errors. Consequently, it could be beneficial to incorporate elevation-dependent weighting of the satellite signals within the shadow-matching algorithm.

As discussed in Section 7.2, GNSS signal propagation prediction using a 3D city model can be highly computationally intensive. This can be mitigated by simplifying the model so that each building is represented by fewer blocks or triangles. This is known as 'generalization' in the geographic information science (GIS) community, i.e., the process by which a map with reduced complexity is derived from a more detailed spatial data source, while retaining the major characteristics of the source data. This will clearly result in increased shadow-matching positioning errors. Therefore, research is needed to determine:

- Acceptable bounds for the 3D model approximation errors, given the other sources of error in shadow matching;
- Which model simplifications have the greatest and least impact on shadow matching (e.g., edges are more important than faces);
- How to simplify the model in such a way that the average impact on shadow-matching performance is minimized.

An extreme form of simplification is the 'urban trench' model [31], whereby all buildings are represented as a pair of continuous walls of equal height, one on each side of the street. This is highly efficient where applicable, but can lead to large errors if used inappropriately.

The real-time computational load can be reduced dramatically using building boundaries [2]. A building boundary is precomputed for each candidate position and describes the minimum elevation above which satellite signals can be received at a series of azimuths. However, converting the 3D city model to a building boundary array introduces additional errors due to the quantisation of the building boundaries. As only discrete azimuths are considered, the boundaries of shadowed regions are effectively shifted to wherever there is a change in the azimuth to which the shadowed region corresponds. The position resolution due to azimuth quantization is $r\Delta\psi$, where $\Delta\psi$ is the azimuth resolution and r is the distance to the building causing the shadowing. Thus, for a 1° azimuth resolution, the position resolution for a building 20m away is 0.35m.

The elevation angle will also be quantized to limit the amount of data required to represent the building boundaries. This results in a position resolution of $h\sin^{-2}\theta\Delta\theta$, where $\Delta\theta$ is the elevation resolution, θ is the elevation angle at the building boundary and h is the building height. For a 1° elevation resolution, 45° elevation, and 20m building height, the position resolution is 0.70m. As the position resolution is poorer for lower elevation angles, it is worth considering storing building boundaries in terms of the sine of the elevation so that lower elevations are quantised less.

Another issue to beware of is differences in datum between the city model (or building boundaries) and GNSS. Mapping is supplied in a local datum that moves with the tectonic plates, whereas GNSS uses a global datum, such as WGS84 or ITRF, that averages out plate movement across the Earth. Therefore, it is necessary to convert either the city model to the global datum or the GNSS positioning to the local datum. A datum conversion for the final position solution may also be required. Any errors in these datum conversions will result in position errors.

An obvious source of errors in shadow matching is out-of-date city models. As 3D mapping is relatively underused, it is not currently updated as frequently as 2D mapping. For example, Ordnance Survey's 2D MasterMap product is updated every 6 weeks. If a building is present in the real world, but absent from the city model, or vice versa, large shadow-matching errors are likely to arise. Mitigating this problem requires a mechanism for maintaining up-to-date city models (see Section 7.3) and the implementation of outlier detection within the shadow-matching algorithm (see Section 5.3). A particular problem is buildings under construction, which can change on a daily basis; a potential solution to this problem is to mark particular regions of the city model (and derivations thereof) as 'do not use' so that signals affected by construction sites are simply omitted from the shadow-matching process.

4.5 Signal Propagation Effects

Basic versions of shadow matching assume that GNSS signal propagation is much simpler than it really is, leading to errors. For example, signals are assumed to be either directly received or completely blocked by buildings. However, real buildings also reflect GNSS signals. Surfaces that are smooth to within about a quarter of a wavelength (~48mm for GPS L1) tend to produce specular reflection, whereas rougher surfaces scatter. Specular reflection produces a strong signal in a particular direction, whereas scattering produces a weak signal across a wide range of angles. Consequently, in dense urban areas, most signals that are not received directly are received via reflection, provided the user equipment is sufficiently sensitive Thus, signals from approximately 40% more satellites were observed with a Samsung Galaxy S3 smartphone than a Leica GS15 geodetic GNSS receiver.

Scattered signals are significantly weaker than directly received signals, so are relatively easy to distinguish using C/N_0. However, specularly reflected signals can be almost as strong as directly received signals. Furthermore, as a result of environmental effects (Section 4.6) and antenna limitations, particularly on smartphones (Section 4.7), some specularly reflected signals can be stronger than some directly received signals. This can confuse the shadow matching algorithm, resulting in a position error. Figure 13 shows an example.

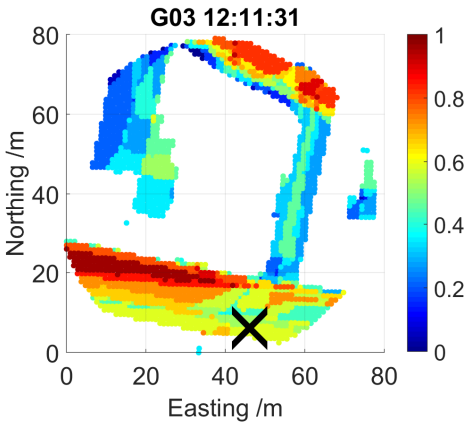

Figure 13: GNSS shadow-matching scoring map with an error due to a specular reflection (the cross shows the true position and white areas are indoor locations)

A potential solution to this problem is to predict reflected signals as well as directly received signals. This is essentially the power matching concept first proposed in [7] and subsequently demonstrated in [13]. However, in [13], it was assumed that all buildings were equally reflective and tests were performed in an environment where this assumption was realistic. In practice, different buildings will exhibit different levels of reflectivity at GNSS wavelengths, depending on the physical and electrical characteristics of their surfaces. Some surfaces absorb more of the signal energy than others. There is also no clear boundary between specular reflection and scattering; a mixture of the two effects can occur. For example, at optical wavelengths, glass and metal buildings exhibit more specular reflection than brick and stone buildings, which mainly scatter. Substantial further research is thus required, including:

- An experimental study into how different types of building reflect GNSS signals, potentially including the testing of different materials in an anechoic chamber;
- Development of an efficient reflectivity prediction method, and
- Enhancement of the shadow matching algorithms to make use of reflection predictions.

A second common approximation is the assumption that the signal path between the satellite and the user antenna is a single ray. The wavelength of GNSS signals (~0.19m for GPS L1) is significant in comparison with buildings. The signal path is therefore determined by the Fresnel zones, such that the effective radius of the signal footprint at a blocking or reflecting object is $\sqrt{r\lambda_{ca}}$, where r is the distance of the object from the user antenna and λ_{ca} is the carrier wavelength. Thus, for a building about 10m away, the diameter of the signal footprint is about 3m. This has two consequences. Firstly, a building can partially block or partially reflect a signal. Secondly, variations in the building surface over the signal footprint can cause both constructive and destructive interference, depending on the angle of incidence. Consequently, a diffraction pattern may be observed as the user and/or satellite move.

In practice, when a GNSS signal is blocked by a building according to the ray approximation, that signal is still receivable if the line of sight to the satellite is within about 5° of the building boundary, either the top or the sides [32]. The signal strength steadily drops as the line of sight moves further behind the building and superimposed on this is a diffraction pattern. An example is shown in Figure 14 [2]. Based on a ray approximation, the satellite was predicted to be directly visible between 9.26 and 9.68 hours. The data was collected in Central London using a Leica Viva GS15 geodetic receiver.

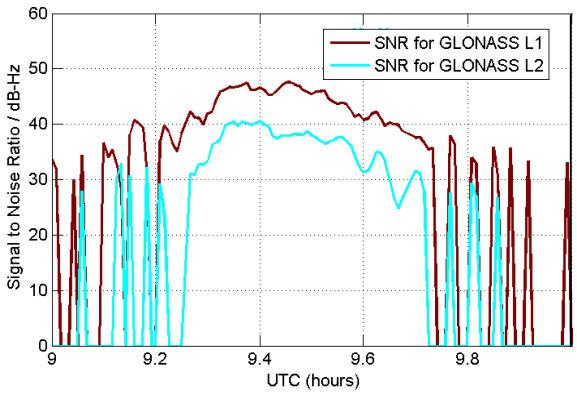

Figure 14: Measured GNSS signal to noise when the signal is partially blocked by a building [2].

The consequence of this for shadow matching is that there is no sharp boundary between regions where a signal can be received and regions where it cannot. Instead, there is a gradual transition. Thus, the wavelength of GNSS signals and their resulting Fresnel radii fundamentally limit the positioning resolution of the shadow matching approach. Further research is needed to determine what this resolution limit is. However, experimental results published by several research groups (see Section 3) suggest that this limit is within 2m. Short of redesigning GNSS to operate at higher frequencies, there is very little that can be done to mitigate this phenomenon as it results from the laws of physics, not the engineering.

Predicting the 'diffraction region' at the edge of buildings was attempted in [11], but this had little effect on shadow-matching performance. Another possibility is to treat these signals as having non-zero probabilities of being both direct LOS and NLOS and computing the matching scores as a weighted average of the two hypotheses. The probabilities used for this weighting could be varied according to how close to the building boundary the predicted line of sight is. This would be consistent with the probabilistic hypothesis scoring requirement discussed in Section 4.8.

4.6 Environmental Complexity

An underlying assumption of shadow matching is that GNSS signals are only affected by the surrounding buildings and other permanent structures. However, the signals are also affected by other objects in the surrounding environment that are impractical to model. Road vehicles can block and reflect GNSS signals. Thus a signal that would normally be direct line of sight could be temporarily blocked, while a strong reflection could be received at locations where a signal is normally weak. High-sided vehicles, such as London's double decker buses, are a particular problem.

Outlier detection (Section 5.3) could be used to minimize the impact of vehicles on shadow matching. Elevation-based signal weighting within the scoring process may also be useful as lower elevation signals are more likely to be affected by vehicles. Similarly, mounting the antenna as high as possible could help, though this is impractical for many applications.

Street furniture, such as bus shelters, vending booths, telephone kiosks and advertising displays will also have an impact though, in principle, this could be incorporated in the 3D city model. Lamp posts are probably too thin to have much of an impact. GNSS signals are also affected by foliage, particularly trees [33]. Foliage attenuates signals with the result that a direct LOS signal could be misclassified as NLOS. It also varies with the season, making it harder to predict.

Radio frequency interference, including deliberate jamming, will also affect shadow matching. Typically, all C/N_0 measurements will be reduced by a common factor. To mitigate this, some form of interference detection is required. Because the noise exceeds the signal strength prior to correlation within the receiver (a common feature of spread spectrum signals), interference can be measured using the receiver front-end. However, making use of this in shadow matching requires the receiver manufacturer to output this information. An alternative is to use the C/N_0 measurements of those signals predicted to be direct LOS throughout the search area to rescale the C/N_0 measurement set.

For vehicle applications, the host vehicle can affect the C/N_0 measurements, particularly where the user antenna is mounted inside. Experiments are thus needed to determine the impact of this.

Finally, GNSS signals are attenuated by the human body, particularly if the antenna is close [34][35]. In the smartphone shadow-matching experiments reported in [16][17], the phone was handheld with the experimenter facing four different 'compass points' at each test site. Shadow matching was successfully demonstrated under these conditions, so body attenuation does not usually prevent it from working. However, its effect on performance needs to be properly quantified.

4.7 Observation Errors

The observation step in shadow matching determines which signals are being received via a direct line-of-sight path and which are not. Clearly, any signal above the masking angle that is not being tracked at all is not receivable via a direct LOS path. Otherwise, the C/N_0 (or signal to noise ratio (SNR)) measurements must be used to determine whether reception is direct LOS or NLOS. In a basic implementation of shadow matching, a simple threshold is used. However, there are several factors that complicate the determination of LOS/NLOS status from C/N_0. These can result in misclassification of signals, potentially resulting in positioning errors.

The first factor is variation in the satellite transmission powers. Each GNSS constellation transmits signals at different powers; while there can also be variations between different generations of satellite within the same constellation. Furthermore, the transmission powers of individual satellites vary, starting out several dB above the nominal level and then gradually decaying with age. An obvious solution is to provide the shadow matching algorithm with the transmission powers of all of the satellites so it can scale the LOS/NLOS detection thresholds accordingly. This information could be distributed with the 3D mapping data (see Section 7.1). Alternatively, the transmission power can be estimated from the C/N_0 measurements taken when each satellite is at a high elevation and predicted to be directly receivable across all high-scoring candidate positions. Algorithms should be developed to do this and should incorporate a long averaging time with outlier detection, but still be responsive to changes as each satellite ages.

The second factor is variation in the user antenna gain pattern. A geodetic-grade antenna has a higher gain than a consumer- or automotive-grade antenna, which in turn has a much higher gain than a smartphone antenna. There can also be variations of a few dB-Hz due to the design of the receiver front-end. A strong direct-LOS signal will exhibit a C/N_0 of more than 40 dB-Hz in a geodetic receiver, such as the Leica Viva series. However, in tests of a Samsung Galaxy S3 smartphone in an open environment, where nearly all signals should be direct LOS, few C/N_0 measurements above 30 dB-Hz were observed [17]. Consequently, different LOS/NLOS detection thresholds are needed for different types of user equipment.

The user antenna gain pattern also varies with the angle of reception. For a typical right-hand-circularly-polarized (RHCP) antenna the gain is highest for signals at normal incidence and drops as the angle of incidence increases. For application where the user antenna remains horizontal, this translates into a variation in antenna gain with the satellite elevation angle, which is known, so this effect can be calibrated and compensated for. Otherwise, it is necessary to maintain a 3D attitude solution in order to perform this compensation.

Smartphones have linearly-polarized antennas, which exhibit significant nulls for signals with lines of sight parallel to the axis of the antenna. The gain varies approximately as the sine of the angle subtended by the antenna axis and the signal line-of-sight vector at the antenna. Signals within a 30° cone are thus attenuated by a factor of 2 (3 dB) or more. As a smartphone may be held at almost any angle, it is not possible to calibrate and compensate for this effect unless a 3D attitude solution is available; this can be difficult to generate using smartphone sensors.

Strong specularly reflected signals are left-hand circularly polarized (LHCP), provided the angle of incidence at the reflector is less than Brewster's angle and the reflector is smooth. A RHCP antenna will attenuate LHCP signals by about 10 dB at normal incidence. This makes it easier to distinguish direct LOS from strong NLOS signals using C/N_0 measurements and minimizes the impact of multipath interference on the C/N_0 of the direct signals. However, the polarization discrimination of a RHCP antenna drops as the angle of incidence increases. For signals incident within its plane, the antenna is effectively linearly polarized and has no polarization discrimination at all. Thus, for a horizontally-mounted antenna, the ability to distinguish between LOS and NLOS signals increases with the satellite elevation angle. This provides further motivation for allocating higher weighting to higher elevation signals within shadow matching's position hypothesis scoring process (Section 4.8) and thus needs further study. Using a dual-polarization (RHCP and LHCP) antenna [36] can improve the sensitivity of LOS/NLOS determination. However, additional receiver hardware is required and the elevation dependency remains. Where a linearly-polarized smartphone antenna is used, there is no gain discrimination between RHCP and LHCP signals. With the nulls in the gain pattern as well, this means that some NLOS signals can be stronger than some direct LOS signals, regardless of the satellite elevation.

The final factor impacting LOS/NLOS determination is how the receiver measures the carrier-power-to-noise-density ratio, C/N_0. Fundamentally, C/N_0 is a measure of postcorrelation signal-to-noise ratio. However, some receivers use precorrelation SNR measurement techniques that only approximate C/N_0, depending on the power spectrum of the noise [37]. Some manufacturers also adjust their SNR measurements to compensate for antenna/receiver losses, whereas others don't. Furthermore, the C/N_0 measurements themselves are subject to noise, which is most significant for weak signals. With a 1s averaging time, the C/N_0 measurement noise SD is about 1 dB-Hz at 20 dB-Hz, increasing to about 3 dB-Hz at 15 dB-Hz [38].

For any GNSS user equipment, it is thus necessary to perform some form of calibration of the C/N_0 threshold(s) for determining LOS/NLOS status to account for the antenna gain, receiver losses and C/N_0 or SNR measurement biases. A universal shadow-matching algorithm that uses the same tuning parameters for all designs of user equipment is thus not feasible, which has implications for server-based shadow matching (Section 7.1). Manual calibration is logistically difficult because of the need to keep up with new products, reliably identify which antenna and receiver is in use, and distribute the calibration parameters.

Self-calibration of the user equipment using high elevation satellites predicted to be directly receivable at all high-scoring candidate positions should be viable where a horizontally mounted RHCP antenna is used. Suitable algorithms should be developed for this, incorporating a long averaging time and outlier detection. This will need to work in collaboration with the satellite transmission power calibration, where implemented, as the two phenomena are difficult to separate. This would leave the variation in antenna gain with incidence angle. If all antennas of a particular class (e.g., geodetic, automotive, etc) have similar gain patterns, it should be possible to use a standard model. Some form of self-calibration may also be possible, particularly if data from open environments is available. However, both approaches require further investigation to assess their feasibility.

For smartphones using linearly polarized antennas, there are the additional problems of the nulls in the antenna gain pattern and the lack of polarization discrimination. Experiments with signals known to be either direct LOS of NLOS have shown that there is significant overlap between their measured C/N_0 distributions [17], noting that some of this variation could be due to user body masking. This is shown in Figure 15. Consequently, if signals are determined to be either direct LOS or NLOS using a simple C/N_0 threshold, the misclassification rate will be too high. For example, using data collected at the same sites, the mean absolute deviation (MAD) of the cross-street shadow-matching position error was found to be 2.1m using a geodetic receiver and 3.9m using a smartphone [16].

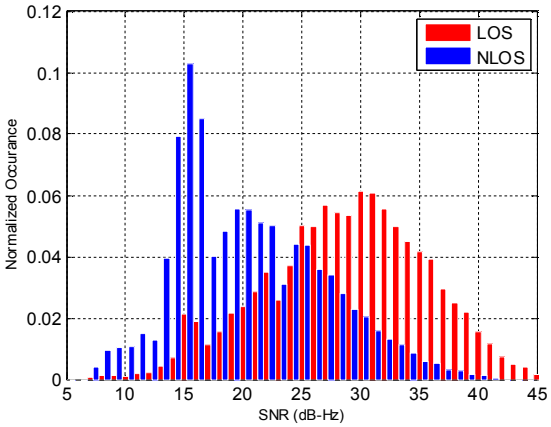

Figure 15: Normalized SNR distributions of LOS and NLOS signals observed using a smartphone across 20 test sites.

In [17], Boolean LOS/NLOS classification on a smartphone is replaced by an estimated probability of each signal being direct LOS, based on the measured C/N_0. This enables the candidate position scoring algorithm to implicitly attribute greater weighting to those signals for which the observed LOS/NLOS status is more certain, resulting in better shadow-matching performance. With more data, there is scope to incorporate satellite elevation into the model for determining the direct LOS probability. Further work is also needed to determine how to adapt the model to different types of smartphone. However, even with better algorithms, shadow matching is never likely to work as well on a smartphone as it will with a RHCP antenna. Moreover, probabilistic LOS/NLOS classification is also likely to be beneficial for shadow matching with a RHCP antenna, noting that different model parameters will be required.

4.8 Hypothesis Scoring and Positioning Algorithms

Shadow matching determines position by comparing the observed and predicted satellite visibility to determine a score for each candidate position hypothesis and then determines a position solution from the scoring grid. Limitations in the algorithms used to do this will result in position errors.

The first limitation is the resolution of the grid of candidate positions within the search area. The majority of shadow-matching tests have used a 1m spacing between candidate positions. A 3m grid spacing was used for the real-time smartphone implementation and produced a position solution about 15% less accurate than with a 1m spacing [15]. One way of balancing performance and processing load is to scale the resolution with the size of the search area so that the number of grid points is fixed. Another option is to initially perform shadow matching with a coarse grid and then add additional grid points in the highest-scoring regions. Whether a higher resolution than 1m would lead to a more accurate position solution depends on the size of the other error sources. At present, it is unlikely to have much effect.

Position hypothesis scoring in shadow matching provides an indication of how likely it is that the user equipment is located at each candidate position. If the observation and prediction phases of shadow matching were perfect, the true position would be one of the highest-scoring candidates and the other candidate positions could be discounted. However, the various errors inherent in the prediction and observation processes (Sections 4.4 to 4.7) effectively add noise to the candidate position scores. Therefore, when the scores of two candidate positions are compared, the difference in those scores must exceed this noise level for there to be confidence that one position is more likely than the other. In other words, the signal-to-noise ratio must be sufficient to extract the underlying signal from the noise.

Improvements to the prediction and observation processes will reduce this noise level. However, noise can never be completely eliminated from GNSS shadow matching as it is not practical to mitigate every source of error. To ensure that the scoring grid is correctly interpreted by the subsequent position determination phase of shadow matching, the sources of error must be understood and quantified so that an appropriate uncertainty can be attributed to each candidate position score.

Ideally, the position hypothesis scoring stage of shadow matching should output a probability distribution, or equivalently a likelihood or log-likelihood surface, noting that likelihood is unnormalized probability. This then enables each candidate position to be correctly weighted using standard statistical techniques when the final position solution is determined; otherwise, position errors will ensue. This is particularly important where shadow matching is combined with other positioning technologies (Section 6), which requires a realistic position uncertainty (see Section 5.1(. Early shadow-matching algorithms have taken a heuristic approach to position scoring. Some simply score 1 where a prediction and observation match and 0 where they do not, while others incorporate different scores for different values of C/N_0.

A first attempt at a probabilistic scoring scheme is described in [16][17]. This uses empirically-derived observed direct-LOS probabilities, but the predicted LOS probabilities are heuristic. Generating realistic probabilities requires identification of all of the major error sources affecting both observation and prediction of direct LOS signals and the acquisition of sufficient experimental data to build an effective model. In practice, this is likely to be an iterative process. Note that a scoring scheme based on probabilities or likelihoods requires the scores from each satellite signal to be multiplied, whereas a log-likelihood-based scoring scheme requires addition of the scores from each satellite.

As discussed in Sections 4.4 and 4.6, lower elevation signals are more difficult to predict accurately and more likely to be affected by unpredictable environmental features, so there is reason to weigh them less in the hypothesis scoring algorithms. Within a probabilistic framework, this can be achieved by allocating a wider range of predicted signal visibilities for high-elevation signals than for low-elevation signals. There may also be merit in adjusting these probabilities according to the building geometry. Section 4.7 also explains that distinguishing direct LOS from NLOS signals using a RHCP antenna is more difficult for low-elevation signals. This effect should be modelled by adjusting the observed signal probabilities.

There are many different ways of extracting a position solution from the shadow-matching scoring grid, resulting in different position errors. Simply taking the highest-scoring candidate position will make the position solution highly sensitive to noise. Taking the average of positions

with scores within a certain margin of the maximum produces a reasonable solution when the matching process is unambiguous, but leads to significant errors where there is an ambiguity [11][17]. The same applies if a weighted average of all candidate positions is taken, noting that this requires probabilistic hypothesis scoring.

The best way to handle an ambiguous scoring grid depends on how the shadow-matching position solution is used. In an integrated system (Section 6.3), information from the other positioning technologies can be used to help resolve the shadow-matching ambiguity [27], so the shadow-matching algorithms should output as much information as possible. This can be the whole scoring grid, expressed as a probability distribution, likelihood surface, or log-likelihood surface. Alternatively, a series of position solution hypotheses can be extracted from the scoring grid, each accompanied by a probability and covariance (Section 5.1). This can be done either by fitting a set of bivariate Gaussian distributions (known as a Gaussian mixture) to the probability distribution/ likelihood surface or by dividing the scoring grid into discrete clusters [39]. Note that the probability of a position hypothesis is proportional to the volume of the corresponding peak in the probability distribution or likelihood surface.

Where a simple single-hypothesis or single-mode integration algorithm, such as an extended Kalman filter (EKF), is used, the shadow-matching solution may simply be rejected whenever it is ambiguous. In this case, shadow-matching could output either the highest-probability position hypothesis (with probability and covariance) or a simple mean and covariance with some measure of ambiguity (Section 5.2).

For a stand-alone shadow-matching system, the requirement may simply be for a "best guess" position, in which case the highest-probability position hypothesis should be output. Alternatively, a confidence region may be required in the form of an ellipse within which there is a certain probability of finding the position (see Section 5.1). In practice, shadow matching will always be integrated with ranging-based GNSS positioning (Section 6.1), so ambiguity could potentially be resolved by multiplying the shadow-matching probability distribution by that of the horizontal ranging-based solution, which is a bivariate Gaussian distribution if a conventional least-squares or EKF positioning algorithm [5] is used. However, this will not always reduce ambiguity and could sometimes increase it. For example, if the ranging solution peak does not coincide with one of the main shadow-matching peaks. A simpler approach is to take the nearest high-scoring position to the initialization position [8]. However, this then makes the shadow-matching position sensitive to errors in the initialization position.

Multi-epoch particle filters combine the shadow-matching scoring grids from successive epochs [13][16][20][21] [22]. Where there is sufficient data, this should normally resolve any ambiguity. However, where the candidate position scores are not true probabilities (or likelihoods), the particle filter may converge too quickly to one candidate position cluster, which may not be the correct one, or continue to consider multiple clusters when there is sufficient data to select one. The position solution will also be sensitive to the tuning of the particle filter itself. In particular, if the particle distribution becomes too tight, the filter can converge on an incorrect solution.

There are (at least) two alternatives to the particle filter for multi-epoch shadow matching. A grid filter maintains an array of equally spaced hypotheses, in contrast to the equal-probability hypotheses of a particle filter. This enables the grid filter's hypotheses to be exactly matched to those of shadow-matching's scoring process, which should be more efficient. A multi-hypothesis Kalman filter (MHKF) [5][40] represents the position solution probability distribution as the sum of a series of multivariate Gaussian distributions (i.e., a Gaussian mixture). This is typically more efficient than a particle filter, particularly where additional states, such as velocity, are added. However, the hypothesis management process can be complex. Multi-epoch filtering can be implemented at a number of levels: shadow matching only, shadow matching plus ranging-based GNSS, and multi-sensor integrated navigation.

One option in an integrated system is to run a multi-epoch shadow-matching filter whenever there is ambiguity. Then, once the filter has processed sufficient epochs to resolve the ambiguity, the shadow-matching position solution can be output to the multisensor integration algorithm and the shadow-matching filter reset. Clearly, considerable research is needed to determine the most efficient position determination and filtering method for shadow matching.

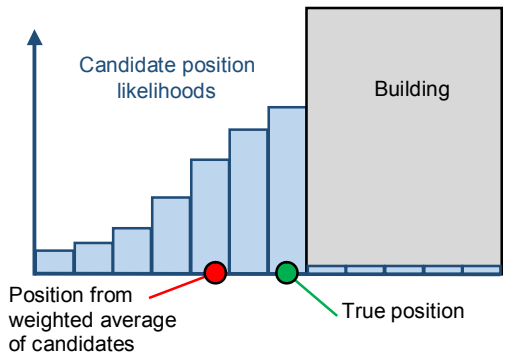

Figure 16: Biasing of the shadow-matching position solution near the edge of a building

A problem that affects all positioning methods is edge effects near buildings. A 3D city model enables indoor areas to be eliminated from the search area. Thus, if the true position is right next to a building, the adjacent candidate positions will have a zero score on the building side and a non-zero score on the street side. Consequently, the application of weighted averaging within the position

determination process will tend to pull the position solution away from the building. Figure 16 illustrates this. This phenomenon will also impact the computation of uncertainty/covariance and the probabilities of different position solution hypotheses. As a systematic error, it should be possible to correct for this phenomenon. However, research will be needed to determine the best method.

5. QUALITY CONTROL

The resolution and degree of ambiguity in the shadow-matching position solution depends on the geometry of the surrounding environment, as explained in Sections 4.1 and 4.2. Shadow matching is also subject to many different error sources (Sections 4.3–4.8). Some of these simply degrade the position accuracy while others introduce completely wrong information into the shadow-matching process. Therefore, like most position-fixing techniques, shadow-matching performance will vary with the location, time, and user equipment. Consequently, to enable shadow matching to be used reliably as part of a practical positioning or navigation system, some form of quality control is required:

- Uncertainty and ambiguity information must be computed to enable subsequent integration and/or application algorithms to treat shadow-matching-derived positioning information with the appropriate weighting. This is discussed in Sections 5.1 and 5.2.
- Outlier detection must be implemented within the shadow-matching process to identify erroneous information and eliminate it form the position solution whenever possible. This is discussed in Section 5.3.

5.1 Uncertainty Determination

Position uncertainty in shadow matching arises from a number of sources, including environmental geometry (Section 4.1), 3D model errors (Section 4.4), and the propagation of GNSS signals (Section 4.5). How this uncertainty is computed depends on the form of the candidate position hypotheses scoring grid and how a position solution is derived from this, as discussed in Section 4.8.

Where the scoring grid is in the form of a probability distribution or likelihood surface, determination of the position uncertainty is straightforward. The 2D position error covariance matrix (from which uncertainty is derived) is obtained simply by computing the second statistical moment of the scoring distribution. Where the distribution has been separated into multiple position hypotheses by clustering, the covariance of each cluster is determined in the same way. Where a set of bivariate Gaussian distributions are fitted to the overall probability distribution, the covariance of each is an output of the fitting process.

Where the candidate position hypothesis scoring in shadow matching is heuristic, an empirical process is required to determine how to extract covariance information from the scoring grid. To ensure these covariances are reliable, experimental data must be collected for as wide a range of operating conditions as possible. Note, however, that a similar empirical process is needed to ensure that the statistical models used to generate a probabilistic scoring grid are reliable.

5.2 Ambiguity Detection

An ambiguous shadow-matching position solution can be caused by a repetitive environment and/or errors in the shadow-matching process. For applications where a single position solution is output (as opposed to a probability distribution or set of hypotheses), it is necessary to indicate when this solution is ambiguous. However, the implications of this ambiguity depend on what kind of position solution is output. If a set of position hypotheses is computed (see Section 4.8) and only the top hypothesis output, then this will be accompanied by a probability which subsequent algorithms can use to determine whether to trust it. If the output position comprises a weighted average of the candidates, an indication of the extent to which the underlying distribution is multimodal would be useful. Approaches to explore include computing and outputting higher order statistical moments (e.g., skew and kurtosis), computing and outputting 95% or 99% confidence error bounds as well as covariance, and simply rescaling the output covariance to compensate for the effects of a multi-modal distribution by ensuring that the shadow-matching solution is downweighted in subsequent processing. Further investigation is needed.

5.3 Outlier Detection

In general, an outlier is a measurement which exhibits a large error due to a fault somewhere. In navigation, a faulty measurement can corrupt the position solution, so a reliable system needs to be able to detect faulty data and either eliminate or correct it [5]. In shadow matching, outliers can occur in both the prediction and observation of satellite visibility. Causes include an out-of-date 3D model (Section 4.4), reception of very strong reflected signals (Section 4.5), the effect of unpredictable objects, such as buses, (Section 4.6), and nulls in the user antenna gain pattern (Section 4.7). These errors can result in contributions from the affected signals to the candidate position hypothesis scoring grid that are completely wrong. Thus, it is desirable to identify the affected signals and remove them from the shadow-matching process.

Fault detection techniques can be divided into range checks, innovation-based methods, consistency checks and infrastructure-based fault detection [5]. Range checks are of little use as visibility prediction will be direct-LOS or NLOS and C/N_0 measurements will be between 10 and 50 dB-Hz regardless of whether outliers are present. Infrastructure-based approaches are limited to mapping updates as the other causes of outliers are local to the

individual user. The discussion here will therefore focus on consistency and innovation-based methods.

Consistency checking of conventional GNSS ranging measurements is normally called receiver autonomous integrity monitoring (RAIM). As well as fault detection and identification (FDI), a full RAIM implementation also incorporates solution protection. However, shadow matching is not sufficiently mature to consider the computation of high-integrity protection levels. Consistency checking techniques for ranging measurements include the solution separation, range comparison, and least-squares residual methods [41]. Equivalents of these techniques for shadow matching are discussed below.

Consistency checking by solution separation computes a set of parallel positioning solutions, each excluding signals from one satellite. If one or more measurements is faulty, these solutions will diverge. However, to identify the faulty signal, solutions excluding two satellites must then be computed so that consistency checking may be performed with each satellite in turn completely excluded. In shadow matching, the underlying causes of outliers will often impact multiple satellites, typically those with similar lines of sight. Consequently, a large number of position solutions, based on different satellite combinations, will be needed for consistency checking. Thus, the processing load could be excessive.

The shadow-matching equivalent of the range comparison and least-squares residual consistency checking methods is to compare each single-satellite candidate position hypothesis scoring grid with a reference scoring grid. The reference grid may be generated from all satellite signals or from all except the satellite under test. However, because outliers can be correlated across multiple satellites with similar lines of sight, it is better to exclude satellites with similar azimuths to the test satellite from the reference grid.

To compare each single-satellite scoring grid with an appropriate reference grid, each grid must first be normalized to zero mean and unit variance, noting that it may be better to compare log-likelihoods than probabilities. A test statistic can then be computed by differencing the normalized scores of the two grids, squaring those differences and then averaging them across all candidate positions, excluding those that are indoors. If the test statistic exceeds a certain threshold, the satellite signal under test can be assumed to be affected by an outlier and excluded from the final position hypothesis scoring grid. The threshold will depend on the scoring scheme and the size of the search area. Signals with borderline test statistics can be downweighted. It may also be useful to consider the sum total of the test statistics for different signals. If this is too high, a viable shadow-matching solution may not be possible.

The shadow-matching equivalent of innovation filtering [5] is to compare each single-satellite scoring grid with a reference grid generated from previous measurements and predicted forward to the current epoch. This is applicable to multi-epoch shadow matching using a particle filter, grid filter, or MHKF (Section 4.8) and the filter can incorporate information from ranging-based GNSS (Section 6.1) and other navigation sensors (Sections 6.2 and 6.3). A key advantage of this approach is that more information is used to generate the reference grid, so it is more sensitive and can operate where there is insufficient information for single-epoch consistency checking. However, there is a risk with innovation filtering (in general) that correct information could be rejected if the navigation filter is allowed to converge to an incorrect solution.

6. INTEGRATION WITH GNSS RANGING AND OTHER SENSORS

Shadow matching will never be implemented on its own in a practical system as the hardware required to implement it can also be used to produce a ranging-based GNSS position solution that is typically complementary to the shadow-matching solution. Furthermore, the 3D mapping used for shadow matching can also be used to improve ranging-based positioning. Where additional navigation and positioning sensors are available, these can be used to aid the shadow-matching process. However, for maximum robustness across different environments and varying host behavior, shadow matching should be deployed as part of a multisensor navigation system. This section discusses each of these topics in turn, followed by a brief discussion of context determination.

6.1 Ranging-based GNSS

As discussed in Section 4.1 and demonstrated experimentally in [11], shadow matching is normally more accurate in the cross-street direction than along the street. Conversely, ranging-based GNSS positioning in a dense urban environment is more accurate along the street because of the geometry of the direct-LOS signals [2]. The two techniques are thus complementary and a better position solution can usually be obtained by combining both solutions, part of the intelligent urban positioning concept. A crude approach is simply to take the cross-street component of the shadow-matching solution and the along-street component of the conventional GNSS solution [28]. However, this does not ensure optimal weighting of the two solutions and is problematic at junctions where there are multiple street directions.

A better way of integrating shadow-matching with ranging-based GNSS is a weighted average of the two solutions based on their covariances. A commercial GNSS position solution does not always come with error covariance information and it is difficult to estimate this from the satellite lines of sight and C/N_0 measurements when details of the receiver's positioning algorithm are

not available. Even where error covariance is supplied, experimental testing is needed to determine whether it can be trusted in dense urban areas. Therefore, it is better to compute the ranging-based position solution within the shadow-matching system, requiring a GNSS receiver that outputs pseudo-ranges.

As discussed in Sections 4.8 and 5, it is difficult to extract a reliable positioning solution and covariance from shadow matching when the candidate position hypothesis scoring grid presents an ambiguous solution. Therefore, integration of shadow matching with ranging-based GNSS at the scoring grid level should be considered. A bivariate Gaussian distribution can be used to determine the likelihood of each candidate position in the scoring grid from the ranging-based position and covariance. The combined score for each candidate position is obtained by multiplying the shadow-matching and ranging scores if they are expressed as probabilities or likelihoods and by adding the two scores if they are expressed as log-likelihoods.

With 3D mapping available, it is a wasted opportunity to integrate a conventional GNSS position solution with shadow matching. Instead, the mapping can be used to improve the ranging-based position solution. For outdoor urban positioning, the height of the user antenna above the ground will typically be known to within half a meter. Therefore, the terrain height from the 3D city model can be used to aid GNSS positioning. The ability of terrain height aiding to improve vertical positioning is well known [5][42]. However, in areas with poor solution geometry, such as dense urban areas, it can also improve the horizontal accuracy by about 40% [43][44][45].

Satellite visibility prediction using a 3D city model enables NLOS signals to be excluded from the ranging-based GNSS solution. Early implementations assumed the user position was approximately known [46][47][48]. However, shadow matching already predicts satellite visibility at every candidate position within the search grid. From this, a NLOS probability across the whole search area can be computed for each satellite and used to weight each pseudo-range measurement within the ranging solution. The NLOS probabilities from the 3D mapping can also be combined with consistency-based and C/N_0-based NLOS prediction techniques, improving the horizontal position accuracy by about 42% compared to a similar approach without the 3D mapping data [45].

Positioning algorithms based on least-squares estimation or an EKF can only use spatially-averaged NLOS predictions. However, a positioning algorithm that scores an array of candidate positions according to the differences between the predicted pseudo-ranges at each point and the measured pseudo-ranges can make different assumptions about which signals are NLOS at each candidate position. The receiver clock error can be eliminated by differencing pseudo-ranges across satellites, while the height of each candidate position can be obtained from the 3D city model's terrain height data. This has the potential to significantly improve positioning performance. Furthermore, the ranging-based and shadow-matching scores for each position on a common scoring grid could easily be combined, helping to reduce the occurrence of ambiguous solutions.

Several research groups have taken this concept of 3D-mapping-aided GNSS ranging a step further by using the 3D city model to predict the path delay of the NLOS signals at each candidate position [49][50][51][52]. A single-epoch positioning accuracy of 4m has been reported [51]. However, the path delay must be determined using ray tracing, which is highly computationally intensive and thus an obstacle to real-time implementation (see Section 7.2). The urban trench approach [31] enables the path delays of NLOS signals to be computed very efficiently, but only if the building layout is highly symmetric. Whether more sophisticated versions of this approach could be developed for more complex building layouts remains a topic for further research.

Figure 17 shows how GNSS ranging and shadow matching could be combined together into an intelligent urban positioning system.

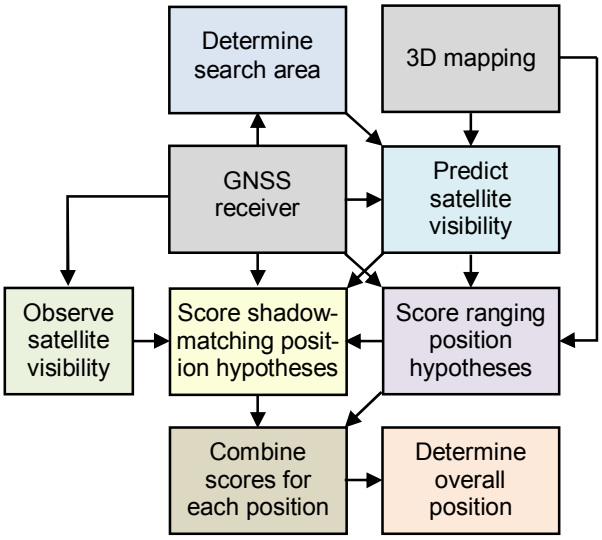

Figure 17: Integration of Shadow Matching with Ranging-Based GNSS

6.2 Aiding from Other Sensors

Other positioning technologies can aid shadow matching in two main ways. The first is through the determination of the search area as discussed in Section 4.3. Wi-Fi positioning is the most practical option. However, any position-fixing technology could potentially be used, whether it is based on radio signals or environmental features [5]. The second opportunity is for multi-epoch shadow matching where an aiding system can be used to determine how much the user has moved between epochs. For pedestrians, a simple step detector can be used to

determine whether or not the user has moved, while pedestrian dead reckoning using step detection can provide an estimate of distance travelled. For vehicles, inertial and magnetic sensors and/or wheel-speed odometry can provide an estimate of speed and distance [5]. However, making a separate shadow-matching or GNSS filter in a multisensor navigation system is not necessarily the most efficient approach.

6.3 Multisensor Navigation and Positioning

To reliably achieve meters-level positioning across a range of different challenging environments, a paradigm shift is needed. Instead of designing a single-technology navigation or positioning system, it is necessary to use as much information as can be cost-effectively obtained from many different sources in order to determine the best possible navigation solution in terms of both accuracy and reliability.

This new approach to navigation and real-time positioning in challenging environments requires many new lines of research to be pursued [27]. These include:

- How to integrate many different navigation and positioning technologies when the necessary expertise is spread across multiple organisations [53];
- How to adapt a multisensor navigation system in real-time to changes in the environmental and behavioural context to maintain an optimal solution [54];
- How to obtain more information for positioning by making use of new features of the environment [55];
- How to handle ambiguous information in a multisensor navigation system;
- How to efficiently distribute environmental data (including 3D mapping).

Thus, in the long term, shadow matching and 3D-mapping-aided GNSS are likely to become just two of many components within a complex multisensor navigation system. The multisensor integrated navigation solution will typically define the search area for shadow matching and 3D-mapping-aided GNSS ranging, while both subsystems will output to an integrated navigation filter, either separately or together. The shadow-matching position data sent to the navigation filter can take a number of forms, as discussed in Section 4.8, and there will be some trade-off between performance and processing load.

6.4 Context Determination

Shadow matching and 3D-mapping-aided GNSS ranging are designed to work in dense urban environments. In open environments, conventional GNSS positioning works well, so the extra processing capacity and mapping data required by advanced GNSS positioning techniques cannot be justified. For indoor environments, it may be possible to enhance GNSS positioning using 3D mapping. However, other positioning technologies, such as Wi-Fi positioning and Bluetooth Low Energy (BLE), are likely to be more effective. Thus, before activating shadow matching and advanced GNSS ranging algorithms, it is necessary to determine the environmental context.

Several studies have shown that GNSS C/N_0 measurements can be used to distinguish indoor, urban, and open environments [56][54][27]. The challenge now is to develop reliable context determination algorithms and assess whether other information, such as Wi-Fi signal strength, ambient light, and magnetic field measurements can be used to assist this process.

7. PRACTICAL ENGINEERING

The final set of challenges that shadow matching must meet are of a more practical nature. These are the design of the overall system architecture, efficient satellite visibility prediction and acquisition of suitable mapping data. This section discusses each of these issues in turn.

7.1 System Architecture

Shadow matching requires GNSS user equipment, a processing platform for the shadow-matching and satellite visibility prediction algorithms, and a means of distributing 3D mapping data. There are two main system architectures that can accommodate this: server-based and receiver-based. In a server-based architecture, the receiver sends pseudo-range and C/N_0 measurements to a remote server which stores all of the mapping data, computes a position solution and sends it to the receiver. In a receiver-based architecture, all processing is done aboard the receiver with the mapping data supplied via a communications link. Both architectures are shown in Figure 18.

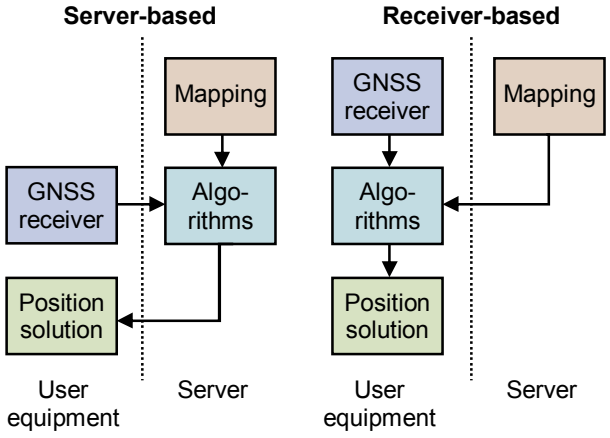

Figure 18: Server-based and receiver-based shadow-matching system architectures

The server-based system architecture has a number of advantages. The user equipment processing load is minimized. Transmitting GNSS measurement data requires minimial communications capacity and existing assisted GNSS (AGNSS) protocols used by mobile phones could be used as C/N_0 measurements are

transmitted from the receiver to the server under the existing 3GPP protocols for server-based positioning [57]. Furthermore, servers can potentially store mapping data for the whole world.

A key disadvantage of a server-based approach is that the time taken to transmit data in both directions, together with potential queuing at the server will introduce a lag in the position computation. This is not a major problem for location-based services, for which data must typically be retrieved from a server anyway. However, it is a potential problem for applications requiring continuous positioning, such as navigation. A second potential problem is the need to calibrate the shadow-matching algorithms to account for the antenna and receiver characteristics (Section 4.7) as this potentially requires a large amount of data to be collected. A possible solution is to transmit model identification data to the server so that calibration data from multiple users of the same type of user equipment can be pooled. Finally, a continuous communications link is required for server-based shadow matching to work, though mobile phone coverage is generally good in dense urban areas.

A receiver-based system architecture potentially offers a shorter processing lag with easier calibration. It is also less reliant on communications continuity as mapping data can be preloaded [10], avoiding the need for any real-time communications. Mapping data could also be exchanged directly between users via peer-to-peer communications, an example of cooperative positioning [27]. Different forms of data distribution could also be combined.

The main challenge of a receiver-based architecture is processing load. Real-time shadow matching has been demonstrated on an Android smartphone [15]. However, the algorithms were simple and the scoring grid resolution was relatively low. A possible way forward is to make use of the graphics processing unit (GPU). A GPU is designed for parallel processing and could potentially run both the satellite visibility prediction and candidate position hypothesis scoring stages of shadow matching. GPUs are accessible for general processing on both PCs and Android phones (but not iPhones, which also fail to provide access to the C/N_0 or SNR measurements that shadow matching requires).

In terms of business models, a server-based architecture leads to the provision of a positioning service. Thus, the suppliers of certain smartphone apps might pay for access to more accurate GNSS positioning, while other apps running on the same device use basic positioning. For the receiver-based architecture, the products are the advanced positioning software and the mapping data. Thus, this approach may be more suited to dedicated navigation and positioning devices. At present, it is recommended that both system architectures be pursued.

A further issue to consider is the GNSS receiver interface. As explained in Sections 4.3 and 6.1, positioning performance will generally be better if pseudo-range measurements can be used. In particular, they enable use of the 3D mapping to aid ranging-based GNSS positioning. However, most consumer-grade and many professional-grade receivers output using the National Marine Electronics Association (NMEA) interface standard, which does not incorporate pseudo-ranges. Some manufacturers add non-standard messages to their NMEA interfaces in order to provide the pseudo-ranges. However, many do not. Thus, the GNSS receiver should be chosen carefully. Interestingly, on smartphones, pseudo-range measurements are available for server-based positioning through AGNSS communications, but are not available through the application programming interface (API) for the use of advanced receiver-based positioning algorithms.

7.2 Signal Prediction

The most computationally intensive part of shadow matching is the satellite visibility prediction. There are three main types of approach. Recursive ray tracing (which may be implemented with standard tools) computes the complete signal path from the satellite to the user antenna. As well as predicting whether or not a signal is receivable via a direct line of sight, it also predicts reflected paths and determines their path delays with respect to the direct path. Recursive ray tracing thus supports the most advanced 3D-mapping-aided GNSS ranging techniques (Section 6.1). However, it is also the most computationally demanding of the three approaches.

The second approach, which is sometimes called ray casting, is intersection based. If the 3D city model is represented as a series of triangles, all triangles within an appropriate region of space are tested to determine whether they block the direct LOS between the user antenna and satellite (halting the search if a blocking triangle is found) [2][11]. A similar approach may be adopted for models comprised of blocks. Representing the city model as an array of block heights on a regularly spaced grid (e.g., 1×1m tiles) can speed up the process at the expense of increased data storage and spatial quantization errors. Intersection techniques are less computationally intensive than ray tracing, but also provide less information.

The third category is projection-based techniques, demonstrated in [8]. These use standard graphics processing tools, implemented on a GPU, to determine in parallel whether the lines of sight from a given satellite to multiple candidate user positions are blocked. An example is shadow mapping [58]. Graphics processing techniques, such as rasterization, can also be used to predict reflections, though not necessarily the associated path delays.

The need to process 3D city models in real time can be eliminated by pre-computing building boundaries [2] at each candidate position using one of the above techniques.

A building boundary describes the minimum elevation above which satellite signals can be received at a series of azimuths. Signal visibility at each candidate position is then determined simply by comparing the satellite elevation angle with that of the building boundary at the satellite azimuth. This is far more efficient in terms of processing load (and hence battery life) than any technique that uses the 3D city model directly and has enabled shadow matching to run on a smartphone.

There is, however, one major disadvantage of building boundaries. They take up much more space than the equivalent city model, requiring more data storage capacity and a higher communications bandwidth for dissemination. A building boundary with a 1° resolution requires about 2500 bits (without compression). For a 100×100m tile with 1m spacing, this corresponds to 3 MB. By contrast, an equivalent array of block heights requires only 12.5 kB. The building boundaries can potentially be compressed more; however, there remains a large difference in the capacity required. Thus, the decision as to whether to use building boundaries or process the city model directly is a trade-off between processing load and data storage load.

7.3 Acquisition of 3D Mapping Data

3D mapping data is become increasingly available and can be generated by a number of methods. Basic LOD 1 3D mapping can now be created cheaply and efficiently using the process of extrusion to "grow" 2D topographic mapping data to a given height, using information from, for example, light detection and ranging (LiDaR)., surveys. This can be achieved within standard Geographical Information Systems, resulting in rapid generation of city-wide datasets suitable for testing shadow matching.

The height information for many 3D city models is derived from LiDAR data. An aerial scan creates a cloud of points by illuminating the scene with a laser array and calculating the distance from the plan based on the reflection time. The denser this resulting point cloud, the higher the accuracy of the height information for individual buildings. In general, three heights are given for each city model: the roof line, the eaves height and the average height of the roof. However, these heights may be inaccurate for lower density point clouds (e.g. 1 point/m^2 versus 1 point/$5m^2$). The selection of height for the LOD 1 model creation will in turn impact the shadow matching process.

More detailed (and realistic) 3D building models are also becoming available, either generated from individual computer aided design (CAD) data, or from terrestrial or airborne LiDaR using dense point clouds to ensure detail is captured. Although this type of model tends to be available mainly for urban, city center, areas, these useful for shadow matching. These LOD 2 models may also be expensive, particularly where texture information is required. For both the flat roofs and more detailed 3D structures, the resulting 3D data is generally quite large in volume and complex in detail [59].

Data availability and coverage itself is also an issue. In the UK it is now possible to obtain building height information for many urban areas, leading to LOD 1 3D data. Ordnance Survey MasterMap data in urban areas is accurate to 0.9m (99% confidence level) [60]. However, this data is expensive, and not universally available in other countries particularly to the same level of horizontal accuracy.

An alternative approach to both of the above problems, although very much in its infancy, is crowd-sourcing of 3D building information, where members of the public capture map data and contribute it to a shared database. GNSS measurements can potentially be used to capture this data [19][20][23][24][25][26], so map building could potentially be incorporated within the shadow-matching system architecture. 3D data capture currently forms part of Open Street Map's worldwide mapping project [61], and, although 3D information is sparse at the moment, this approach shows promise for the future should it mirror the growth of the equivalent 2D Map.

8. SUMMARY

This paper has summarized the state of the art of shadow matching, presented the first comprehensive review of its error sources, and proposed a program of research and development to take the technology from proof of concept to a robust, reliable and accurate urban positioning product.

The tasks ahead may be grouped into three categories: error characterization, algorithm development and systems engineering. They are summarized below.

To quantify the error sources of shadow matching and assess how the performance varies under different operating conditions, the following should be investigated experimentally:

- The effects of building geometry and distribution, scale, roof type, building height to street width ratio, and street direction;
- The effect of building surface characteristics (e.g. glass/steel vs brick stone);
- The effects of passing vehicles, street furniture, vegetation, passing people, a host vehicle and the user's body;
- The effect of varying the user antenna and GNSS receiver;
- The physical limit to shadow matching resolution imposed by the signal wavelength and how this impacts the highest useful matching grid resolution;
- The effects of 3D city model errors, including level of detail, resolution and roof detail;
- The errors that arise when positioning very close to buildings.

To improve the performance of shadow matching, the following algorithm development should be conducted:

- Determination of the optimum search area and region of interest;
- Calibration of the satellite transmission power, user antenna gain and receiver characteristics;
- Development of interference detection and mitigation algorithms;
- Incorporation of reflected signal prediction;
- Incorporation of elevation-dependent signal weighting in the scoring process;
- Development of a fully probabilistic scoring scheme, comprising both predictions and observations, for the candidate position hypotheses;
- Correction of the positioning bias close to buildings;
- Incorporation of quality control including uncertainty computation, ambiguity detection, and outlier detection;
- Extraction of multiple position solution hypotheses with associated probabilities and covariances from the scoring grid;
- Determination of the best multi-epoch positioning algorithm, comparing the grid filter and MHKF with the particle filter;
- Integration of shadow matching with ranging-based GNSS and other navigation sensors.

To enable shadow matching to be deployed in professional and consumer products, the following systems engineering tasks should be completed:

- Build prototypes of both a server-based shadow matching system architecture and a receiver-based architecture with real-time data dissemination to assess the practicality of each approach;
- Work with GNSS receiver manufacturers to develop standard interfaces for both server-based and receiver-based shadow matching to ensure that both C/N_0 and pseudo-range measurements are readily available (or, alternatively, develop a mapping data interface to enable shadow matching to run on a GNSS chipset);
- Determine the optimum satellite visibility prediction technique and mapping data format (including compression) for shadow matching, balancing accuracy, processing load, and data storage requirements. This may or may not use building boundaries as an intermediary;
- Determine the most effective way of sourcing 3D mapping for shadow matching, considering cost, accuracy, availability and maintainability.

ACKNOWLEDGEMENTS

This work is funded by the Engineering and Physical Sciences Research Council (EPSRC) project EP/L018446/1, *Intelligent Positioning in Cities using GNSS and Enhanced 3D Mapping*. The project is also supported by Ordnance Survey, UBlox and the Royal National Institute for Blind People.

The paper includes some results from Dr Lei Wang's PhD research. This was jointly funded by the University College London Engineering Faculty Scholarship Scheme and the Chinese Scholarship Council. The authors would like to thank Prof. Marek Ziebart (UCL) for his support of this project.

Finally, the authors would like to thank Haraldur Gunnarsson of UCL for his comments and suggestions.

REFERENCES

[1] Groves, P. D., "Shadow Matching: A New GNSS Positioning Technique for Urban Canyons". *Journal of Navigation*, 64(3), 2011, 417-430. Also available from http://discovery.ucl.ac.uk/.

[2] Wang, L., Groves, P. D. and Ziebart, M. K., "Multi-Constellation GNSS Performance Evaluation for Urban Canyons Using Large Virtual Reality City Models," *Journal of Navigation*, 65(3), 2012, 459–476. Also available from http://discovery.ucl.ac.uk/.

[3] Bradbury, J., Ziebart, M., Cross, P. A., Boulton, P. & Read, A., "Code Multipath Modelling in the Urban Environment Using Large Virtual Reality City Models: Determining the Local Environment". *Journal of Navigation,* 60(1), 2007, 95-105.

[4] Suh, Y. and Shibasaki, R.., "Evaluation of satellite-based navigation services in complex urban environments using a three-dimensional GIS". *IEICE Transactions on Communications,* E90-B**,** 2007, 1816-1825.

[5] Groves, P. D., *Principles of GNSS, inertial, and multi-sensor integrated navigation systems*, Second Edition, Artech House, 2013.

[6] Tiberius, C. & Verbree, E., "GNSS positioning accuracy and availability within Location Based Services: The advantages of combined GPS-Galileo positioning." *ESA NaviTec* 2004.

[7] Saab, S., & Kassas, Z., "Power matching approach for GPS coverage extension". *IEEE Trans. on Intelligent Transportation Systems*, 7(2), 2006, 156–166.

[8] Ben-Moshe, B., et al., "Improving Accuracy of GNSS Devices in Urban Canyons". *23rd Canadian Conference on Computational Geometry*, 2011.

[9] Wang, L., Groves, P. D. and Ziebart, M. K., "GNSS Shadow Matching Using A 3D Model of London". *European Navigation Conference*, London, 2011. Also available from http://discovery.ucl.ac.uk/.

[10] Groves, P. D., L. Wang, and M. K. Ziebart, "Shadow Matching: Improved GNSS Accuracy in Urban Canyons," *GPS World*, February 2012. Also available from http://discovery.ucl.ac.uk/.

[11] Wang, L., Groves, P. D. and Ziebart, M. K., "GNSS Shadow Matching: Improving Urban Positioning Accuracy Using a 3D City Model with Optimized Visibility Prediction Scoring". *NAVIGATION*, 60(3), 2013, 195–207. (First published at *ION GNSS,* 2012, Nashville, TN). Also available from http://discovery.ucl.ac.uk/.

[12] Yozevitch, R., Ben-Moshe, B., and Levy, H., "Breaking the 1 meter accuracy bound in commercial GNSS devices," *IEEE 27th Convention of Electrical and Electronics Engineers in Israel*, 2012.

[13] Suzuki, T., and Kubo, N., "GNSS Positioning with Multipath Simulation using 3D Surface Model in Urban Canyon". *ION GNSS* 2012, Nashville, TN.

[14] Wang, L, Groves, P. D., and Ziebart, M. K., "Shadow Matching: Improving Smartphone GNSS Positioning in Urban Environments" CSNC 2013 Proceedings, Lecture Notes in Electrical Engineering 245, 2013, 613-621. Also available from http://discovery.ucl.ac.uk/.

[15] Wang, L., Groves, P. D. and Ziebart, M. K., "Urban Positioning on a Smartphone: Real-time Shadow Matching Using GNSS and 3D City Models". *ION GNSS+ 2013*. Nashville, Tennessee. AND *Inside GNSS*, Nov/Dec 2013, 44–56. Also available from http://discovery.ucl.ac.uk/.

[16] Wang, L., *Investigation of Shadow Matching for GNSS Positioning in Urban Canyons*, PhD Thesis, University College London, 2015. Available from http://discovery.ucl.ac.uk/.

[17] Wang, L., Groves, P. D. and Ziebart, M. K., "Smartphone Shadow Matching for Better Cross-street GNSS Positioning in Urban Environments". *Journal of Navigation*, 68(3), 2015, 411–433. Also available from http://discovery.ucl.ac.uk/.

[18] Yozevitch, R., Ben-Moshe, B. & Dvir, A., "GNSS Accuracy Improvement Using Rapid Shadow Transitions". *IEEE Transactions on Intelligent Transportation Systems*, PP (99), 2014, 1-10.

[19] Isaacs, J. T., Irish, A. T., et al., "Bayesian localization and mapping using GNSS SNR measurements". *IEEE/ION PLANS* 2014. Monterey, California.

[20] Irish, A. T., Isaacs, J. T., et al., "Belief Propagation Based Localization and Mapping Using Sparsely Sampled GNSS SNR Measurements," *IEEE International Conference on Robotics & Automation*, 2014. Hong Kong, China.

[21] Wang, L., "Kinematic GNSS Shadow Matching Using a Particle Filter", *ION GNSS+* 2014. Tampa, Florida. Also available from http://discovery.ucl.ac.uk/.

[22] Yozevitch, R. and Ben-Moshe, B., "A Robust Shadow Matching Algorithm for GNSS Positioning," *NAVIGATION*, 62(2), 2015.

[23] Swinford, R. P. ''Building on-the-fly world models for pervasive gaming and other ubicomp applications using GPS availability data,'' *IEE International Workshop on Intelligent Environments*, 2005, Colchester, UK, 133–142.

[24] Kim, K., et al., "Localization and 3D reconstruction of urban scenes using GPS", *IEEE Symposium on Wearable Computers*¸ 2008.

[25] Weissman, A., Ben-Moshe, B., Levi, H., and Yozevitch, R., "2.5D mapping using GNSS signal analysis", *Workshop on Positioning, Navigation and Communication*, 2013.

[26] Irish, A. T., Isaacs, J. T., et al., "Probabilistic 3D Mapping based on GNSS SNR Measurements," *IEEE International Conference on Acoustics, Speech and Signal Processing*, 2014.

[27] Groves, P. D., et al., "The Four Key Challenges of Advanced Multisensor Navigation and Positioning", *IEEE/ION PLANS* 2014. Monterey, California. Also available from http://discovery.ucl.ac.uk/.

[28] Groves, P. D., Jiang, Z., Wang, L. and Ziebart, M., "Intelligent Urban Positioning using Multi-Constellation GNSS with 3D Mapping and NLOS Signal Detection". *ION GNSS* 2012. Nashville, Tennessee. Also available from http://discovery.ucl.ac.uk/.

[29] OGC 2015, *CityGML Standard, Open Geospatial Consortium*, http://www.opengeospatial.org/standards/citygml [Accessed 3rd February 2015]

[30] Kolbe, T. H., Groger, G. and Plumer, L., "CityGML: Interoperable access to 3D city models." In: *Geo-information for disaster management*, Springer, 2005, 883–899.

[31] Betaille, D., et al., "A New Modeling Based on Urban Trenches to Improve GNSS Positioning Quality of Service in Cities". *IEEE Intelligent Transportation Systems Magazine*, 5(3), 2013, 59–70.

[32] Bradbury, J., "Prediction of Urban GNSS Availability and Signal Degradation Using Virtual Reality City Models," *Proc. ION GNSS 2007*. Fort Worth, TX.

[33] Spilker, J. J., Jr., "Foliage Attenuation for Land Mobile Users," In *Global Positioning System: Theory and Applications Volume I*, B. W. Parkinson and J. J. Spilker, Jr., (eds.), Washington, DC: AIAA, 1996, 569–583.

[34] Bancroft, J. B., et al., "Observability and Availability for Various Antenna Locations on the Human Body," *Proc. ION GNSS 2010*, Portland, OR.

[35] Bancroft, J. B., et al., "GNSS Antenna-Human Body Interaction," *Proc. ION GNSS 2011*, Portland, OR.

[36] Jiang, Z. and Groves, P. D., "NLOS GPS signal detection using a dual-polarisation antenna", *GPS Solutions*, Vol. 18(1), 2014, 15-16, DOI:

10.1007/s10291-012-0305-5. Also available from http://discovery.ucl.ac.uk/.

[37] Betz, J. W., "Effect of Partial-Band Interference on Receiver Estimation of C/N0: Theory," *Proc. ION NTM*, Long Beach, CA, January 2001.

[38] Groves, P. D., "GPS Signal to Noise Measurement in Weak Signal and High Interference Environments," *NAVIGATION*, 52(2), 2005, 83–92.

[39] Groves, P. D., Handley, R. J., and Runnalls, A. R., "Optimising the Integration of Terrain Referenced Navigation with INS and GPS," *Journal of Navigation*, 59(1), 2006, 71–89.

[40] Reid, D. B., "An Algorithm for Tracking Multiple Targets," *IEEE Trans. on Automatic Control*, AC-24, 1979, 843–854.

[41] Brown, R. G., "Receiver Autonomous Integrity Monitoring," In *Global Positioning System: Theory and Applications Volume II*, B. W. Parkinson and J. J. Spilker, Jr, (eds.), Washington, DC: AIAA, 1996, 143–165.

[42] Amt, J. R. and Raquet, J. F., "Positioning for Range-Based Land Navigation Systems Using Surface Topography," *Proc. ION GNSS* 2006, Fort Worth, TX, 1494–1505.

[43] Groves, P. D. and Jiang, Z., "Height Aiding, C/N0 Weighting and Consistency Checking for GNSS NLOS and Multipath Mitigation in Urban Areas". *Journal of Navigation*, 66, 2013, 653–669. Also available from http://discovery.ucl.ac.uk/.

[44] Adjrad, M., Groves, P. D., and Ellul, C., "Enhanced GNSS Positioning with 3D Mapping", *International Navigation Conference*, 2015, London, UK. Also available from http://discovery.ucl.ac.uk/.

[45] Adjrad, M. and Groves, P. D., "Enhancing Conventional GNSS Positioning with 3D Mapping without Accurate Prior Knowledge", *ION GNSS*+ 2015, Tampa, FL. Also available from http://discovery.ucl.ac.uk/.

[46] Obst, M., S. Bauer, and G. Wanielik, "Urban Multipath Detection and mitigation with Dynamic 3D Maps for Reliable Land Vehicle Localization," *IEEE/ION PLANS* 2012.

[47] Bourdeau, A. and Sahmoudi, M., "Tight Integration of GNSS and a 3D City Model for Robust Positioning in Urban Canyons". *ION GNSS* 2012. Nashville, Tennessee.

[48] Peyraud, S., et al., "About Non-Line-Of-Sight Satellite Detection and Exclusion in a 3D Map-Aided Localization Algorithm," *Sensors*, Vol. 13, 2013, pp. 829-847.

[49] Suzuki, T., and Kubo N., "Correcting GNSS Multipath Errors Using a 3D Surface Model and Particle Filter," *ION GNSS*+ 2013, Nashville, TN.

[50] Kumar, R. and Petovello, M, G., "A Novel GNSS Positioning Technique for Improved Accuracy in Urban Canyon Scenarios using 3D City Model", *ION GNSS*+ 2014, Tampa, FL.

[51] Hsu, L.-T., Gu, Y., and Kamijo, S., "3D building model-based pedestrian positioning method using GPS/GLOANSS/QZSS and its reliability calculation", *GPS Solutions*, 2015, doi 10.1007/s10291-015-0451-7.

[52] Hsu, L.-T., Gu, Y., and Kamijo, S., "NLOS Exclusion using Consistency Check and City Building Model in Deep Urban Canyons", *ION GNSS*+ 2015, Tampa, FL.

[53] Groves, P. D., "The Complexity Problem in Future Multisensor Navigation and Positioning Systems: A Modular Solution," *Journal of Navigation*, 67(3), 2014, 311–206. Also available from http://discovery.ucl.ac.uk/.

[54] Groves, P.D., H. Martin, K. Voutsis, D. Walter, and L. Wang, "Context Detection, Categorization and Connectivity for Advanced Adaptive Integrated Navigation," *Proc. ION GNSS*+ 2013, Nashville, TN. Also available from http://discovery.ucl.ac.uk/.

[55] Walter, D. J., Groves, P. D., Mason, R. J., Harrison, J., Woodward, J. and Wright, P., "Road Navigation Using Multiple Dissimilar Environmental Features to Bridge GNSS Outages," *Proc. ION GNSS*+ 2015, Tampa, FL. Also available from http://discovery.ucl.ac.uk/.

[56] Lin, T., C. O'Driscoll, and G. Lachapelle, "Development of a Context-Aware Vector-Based High-Sensitivity GNSS Software Receiver," *Proc. ION ITM*, Jan. 2011.

[57] ETSI 3GPP, *Digital cellular telecommunications syste, (Phase 2+); Location Services (LCS); Mobile Station (MS) – Serving Mobile Location Centre (SMLC) Radio Resource LCS Protocol (RRLP)*, Technical Specification TS 44.031 version 12.2.0 Release 12, April 2015.

[58] Akenine-Möller, T., Haines, E., and Hoffman, N., *Real-Time Rendering*, 3rd Edition, A. K. Peters Ltd, Natick, MA, USA, 2008.

[59] Glander, T. and Dollner, J., "Techniques for generalizing building geometry of complex virtual 3D city models". In: *Advances in 3D Geoinformation Systems*, Springer, 2008, 381–400.

[60] Ordance Survey, *Mastermap Topography Later Support*, http://www.ordnancesurvey.co.uk/business-and-government/help-and-support/products/topography-layer.html (accessed 2nd June 2015)

[61] Haklay, M., and Weber, P.,"Openstreetmap: User-generated street maps". *Pervasive Computing, IEEE*, *7*(4), 2008, 12-18